In Situ Attenuated Total Reflection Infrared Spectroscopy of Dendrimer-Stabilized Platinum Nanoparticles Adsorbed on Alumina

Dongxia Liu,[†] Jinxin Gao,[‡] Catherine J. Murphy,[‡] and Christopher T. Williams*,[†]

Department of Chemical Engineering, Swearingen Engineering Center, University of South Carolina, Columbia, South Carolina 29208, and Department of Chemistry and Biochemistry, University of South Carolina, Columbia, South Carolina 29208

Received: March 12, 2004; In Final Form: May 7, 2004

The adsorption of PAMAM G4OH dendrimer and dendrimer-stabilized platinum nanoparticles onto alumina supports has been investigated using in situ attenuated total reflection infrared (ATR−IR) spectroscopy. The presence of dendrimers on the Al_2O_3 surface is indicated by the appearance of several characteristic vibrational bands. The positions and relative intensities of amide I and II bands suggest that dendrimer conformation is effected by the presence of the encapsulated platinum nanoparticle. Aqueous phase carbon monoxide adsorption onto supported encapsulated Pt nanoparticles results in the appearance of a prominent vibrational peak associated with terminally adsorbed CO. The adsorbed CO can be removed by purging the CO from the liquid with either dissolved O_2 or N_2. The mechanism for this removal is likely via a reaction of CO with adsorbed OH formed from water dissociation. Comparisons with a traditional supported 1% Pt/γ-Al_2O_3 catalyst indicate that the surrounded dendrimer does not hinder the adsorption of CO on the Pt when liquid water is present. However, under dry conditions the dendrimer completely blocks the occurrence of any CO adsorption.

Introduction

Dendrimers[1−3] are monodisperse, hyper-branched polymers that emanate from a central core with repetitive branching units. While possessing a very dense exterior, they contain hollow pockets that can be ideal for use as nanoscale containers. The use of dendrimers as templates/stabilizers for synthesis of encapsulated nanoparticles is a relatively new but active field.[4−18] One of the more successful applications along these lines has been the synthesis of metal nanoparticles using poly(amidoamine) (PAMAM) dendrimers. Originally pioneered by Crooks et al.,[4] the approach takes advantage of the fact that transitional metal ions (e.g., Pt^{2+}, Cu^{2+}, and Pd^{2+}) can coordinate with the interior amine groups of the dendrimer. Such ions may then be reduced to form encapsulated metal nanoparticles that are stable for extended periods of time. Metal nanoparticles synthesized in this fashion have been demonstrated to exhibit interesting catalytic properties.[4−14] The dendrimer can exert control over size and (in the case of multiple metal ions) composition of nanoparticles, which can allow for tuning of catalytic properties. Furthermore, it has been shown that the dendrimer can function as a size-selective barrier during liquid-phase reactions.[19] Most of the reported catalytic studies have been homogeneous,[6] in that the dendrimer−metal nanoparticles have been used directly in solution. Designing a heterogeneous analogue requires the ability to anchor these catalysts onto high-surface-area supports such as oxides.

Attachment of dendrimers onto various surfaces has been well studied, and several strategies have been developed, such as direct adsorption,[20−23] covalent linkage,[24−26] and electrostatic attachment.[27,28] However, there is much less known about the delivery of dendrimer-stabilized metal nanoparticles to surfaces. In this article, we report an attenuated total reflection infrared (ATR−IR)[29] spectroscopic study of the adsorption of hydroxyl-terminated generation 4 PAMAM dendrimers and dendrimer-stabilized platinum nanoparticles onto an alumina support in aqueous solution. The results suggest that dendrimer-platinum nanocomposites are very strongly adsorbed on the oxide surface and that the platinum nanoparticle remains accessible to liquid-phase species.

Experimental Section

Materials. Carbon monoxide (UHP), oxygen (UHP), and nitrogen (UHP) were obtained from National Welders and used as received. Hydroxyl-terminated fourth-generation (G4OH) poly(amidoamine) (PAMAM) dendrimer was obtained as 10 wt % methanol solution (Aldrich). Prior to use, the methanol was removed from the dendrimer using flowing N_2 at room temperature. K_2PtCl_4 (99.99%), H_2PtCl_6 (99.5%, Premion), and $NaBH_4$ (98%) were purchased from Aldrich. Gamma aluminum oxide powder (99.5%, metal basis) was obtained from Alfa Aesar. Ultrapure deionized (18 MΩ) water was used for all sample preparations and adsorption experiments.

Synthesis. Dendrimer-stabilized platinum nanoparticles were synthesized using a method adapted from the literature,[7] which has been described previously.[30] Briefly, equal volumes of aqueous 0.2 mM PAMAM G4OH and 8.0 mM K_2PtCl_4 solutions are mixed together, yielding a Pt^{2+}-to-dendrimer ratio of 40:1. The mixed solution is stirred for 10 days, resulting in a color change from faint to strong yellow. The resulting Pt^{2+}-G4OH solution was subsequently reduced with an equal volume of fresh 32 mM $NaBH_4$ (98%, Aldrich) solution and stirred for at least 1 h. The final solution of 0.05 mM PAMAM G4OH/Pt40 was purified by dialysis for 2 days against pure deionized

* To whom correspondence should be addressed: Christopher T. Williams, Department of Chemical Engineering, Swearingen Engineering Center, University of South Carolina, Columbia, SC 29208. Fax: (803) 777−8265. E-mail: willia84@engr.sc.edu.

[†] Department of Chemical Engineering, University of South Carolina.

[‡] Department of Chemistry and Biochemistry, University of South Carolina.

10.1021/jp048879i CCC: $27.50
Published on Web 08/04/2004

water (Milli-Q) using cellulose tubing with a 1200 dalton cutoff (Sigma-Aldrich). Atomic force microscopy studies of the nanoparticle size distribution[30] show that 80% of the nanoparticles in solution have an average particle size of around 0.7 nm and reside within the individual dendrimers. The remaining 20% of particles have sizes varying from 1 to 3 nm and appear to be external to the dendrimer core. Nevertheless, they appear to be stabilized (i.e., through arrested precipitation) by the external surfaces of dendrimer molecules.

For comparison purposes in molecular adsorption studies, a 1 wt % Pt/γ-Al_2O_3 catalyst was prepared using standard wet (aqueous) impregnation with H_2PtCl_6 as the precursor. The γ-Al_2O_3 support has a mean particle size of 37 nm and a surface area of 45 m^2/g as given by the manufacturer (and measured in our laboratory using the BET method). The dried impregnated support was calcined in O_2 at 500 °C for 3 h and reduced in H_2 for 2 h at 300°C.

In Situ ATR−IR Measurements. The details of the setup for performing in situ ATR−IR studies of alumina powder films have been described previously.[31] In short, γ-Al_2O_3 powder or 1 wt % Pt/γ-Al_2O_3 catalyst is deposited from an aqueous suspension onto a trapezoidal Ge waveguide. The substrate is then placed in a homemade flow cell that mounts onto an ATR−IR accessory (SpectraTech) within the FTIR spectrometer (Nicolet Nexus 670). The alumina film is allowed to equilibrate under flowing deionized water for at least 8 h prior to exposure to low concentration (i.e., <40 μM) aqueous solutions of dendrimer or dendrimer-stabilized Pt nanoparticles. Dendrimer concentration in the system was controlled by stepwise injection of stock solution into a water reservoir, which is pumped through the flow cell. Gas (i.e., N_2, O_2, CO) was introduced to the adsorbed dendrimers by sparging through the external liquid reservoir. All measurements were performed at room temperature of 25 °C.

Results and Discussion

Figure 1 shows typical bulk-phase ATR−IR spectra obtained for 50 μM aqueous G4OH (bottom) and 50 μM aqueous G4OH/Pt40 (top). These spectra were obtained by first acquiring a background spectrum of 0.6 mL of pure water in contact with the bare Ge waveguide. After switching to the same volume of the dendrimer solution, a spectrum was obtained that was referenced to this water background. This procedure resulted in a spectrum largely devoid of any significant contributions from liquid water. The G4OH spectrum exhibits two broad peaks centered at 1637 and 1560 cm^{-1} that are readily assigned, respectively, to the C═O stretching (amide I) and N−H bending/C−N stretching (amide II) vibrations of the dendrimer.[32] In addition, the weak features clustered around ca. 1450 cm^{-1} are assigned to CH_2 scissoring vibrations.[11,32]

The spectrum of G4OH/Pt40 exhibits markedly different characteristics. While the amide II band position is almost identical to that in G4OH, there is a ca. 10 cm^{-1} upshift in the amide I frequency. This strongly suggests a direct interaction of the C═O bonds in G4OH with the Pt nanoparticle surface. In contrast, a recent FTIR study of dendrimer-stabilized gold and silver nanoparticles exhibited a more pronounced interaction with the C−N bond, which manifested itself through a blue shift in the amide II vibration.[11] Nevertheless, a similar frequency blue shift in the amide I vibration has been observed with FTIR for amide C═O bonds in peptides interacting with a Cu(110) surface.[33] Thus, the nature of the interaction appears to depend strongly on the type of metal being encapsulated. In addition to this significant *chemical* interaction, the amide I:amide II intensity ratio is altered from about 3:2 to 2:3 in the presence of the Pt nanoparticle. Such a ratio shift may be analogous to what is observed during FTIR studies of protein secondary structure, where the amide I and amide II band intensities are known to change with the degree of alpha helix and beta sheet conformations, which in turn is dependent on the surrounding environment.[34−37] In the present case, it is likely that the platinum nanoparticle is occupying space and prevents hydrogen bonding between the branches of the dendrimer. However, more extensive infrared measurements coupled with molecular simulation calculations would be required to confirm this hypothesis.

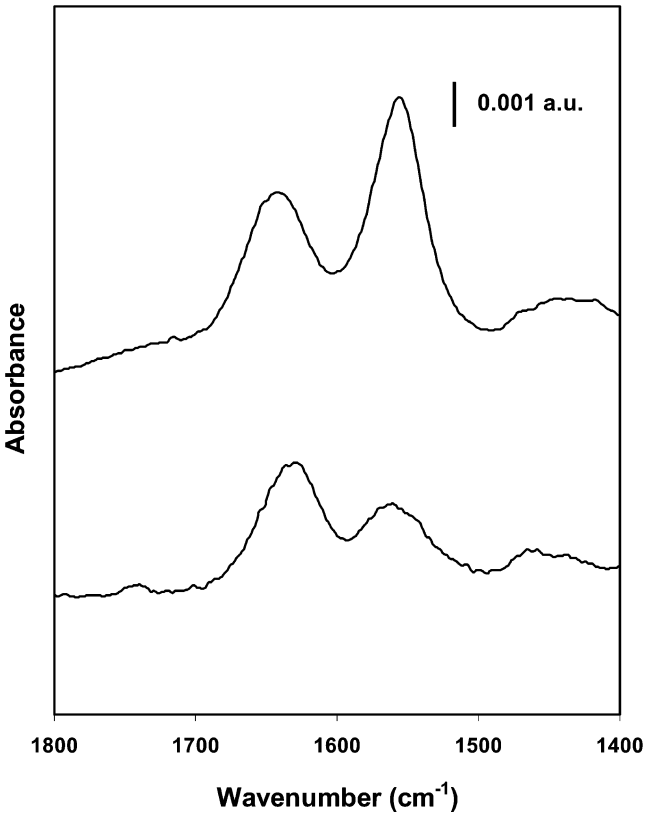

Figure 1. Bulk ATR−IR spectra of aqueous 0.05 mM G4OH (bottom) and aqueous 0.05 mM G4OH/Pt40 (top).

Figure 2 shows representative ATR−IR spectra for adsorption of PAMAM G4OH on alumina in water. The bottom spectrum (a) was acquired before adding the dendrimer to the solution. Except for a small, broad feature at ca. 1645 cm^{-1} resulting from incomplete background subtraction of liquid water, there are no other peaks present. Dendrimer solution was injected into the flowing system to reach a final concentration of 37.5 μM. After exposure to this concentration for 1 h, the system was purged with pure water and a spectrum was taken after 12 min (spectrum b). The G4OH is clearly adsorbed on the surface, as evidenced by the amide I (1637 cm^{-1}) and II (1560 cm^{-1}) peaks that are essentially unchanged in frequency. While the dendrimer is readily adsorbed on the alumina under the whole range of concentrations studied (i.e., 1.96−37.5 μM), prolonged exposure to pure water resulted in gradual desorption. For example, after another 10 h of rinsing (spectrum c), the intensities of the dendrimer peaks have decreased by about 20%.

The adsorption of PAMAM G4OH/Pt40 on alumina reveals different behavior. Figure 3 shows a set of spectra for adsorption from a 4.54 μM solution. The spectrum (a) acquired just prior to addition of G4OH/Pt40 is devoid of features, except again for a small water peak arising from incomplete subtraction. After

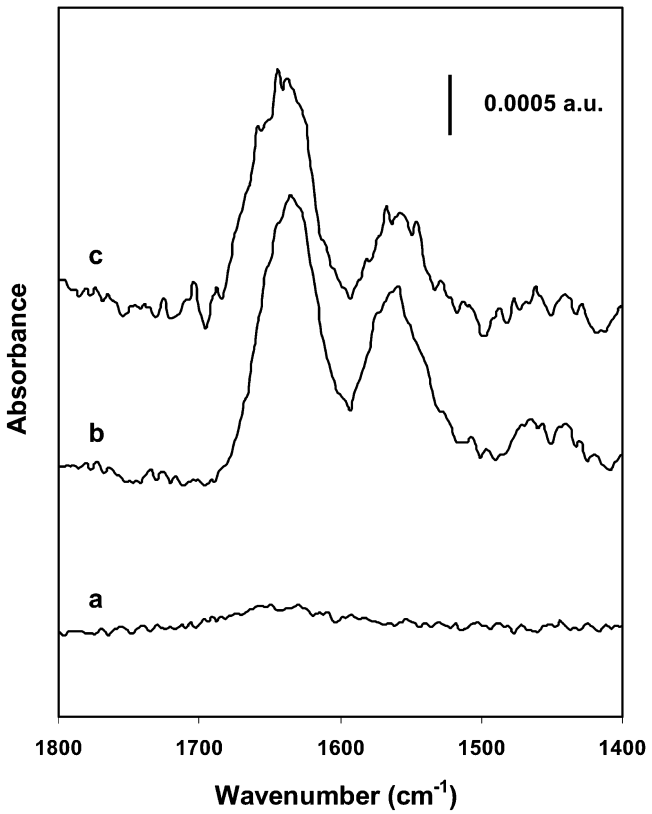

Figure 2. In situ ATR−IR spectra of an alumina film (a) after saturation with water, (b) after exposure to 37.5uM G4OH solution for 1 h followed by 12 min rinsing with water, and (c) after continued rinsing for 10 h. See text for details.

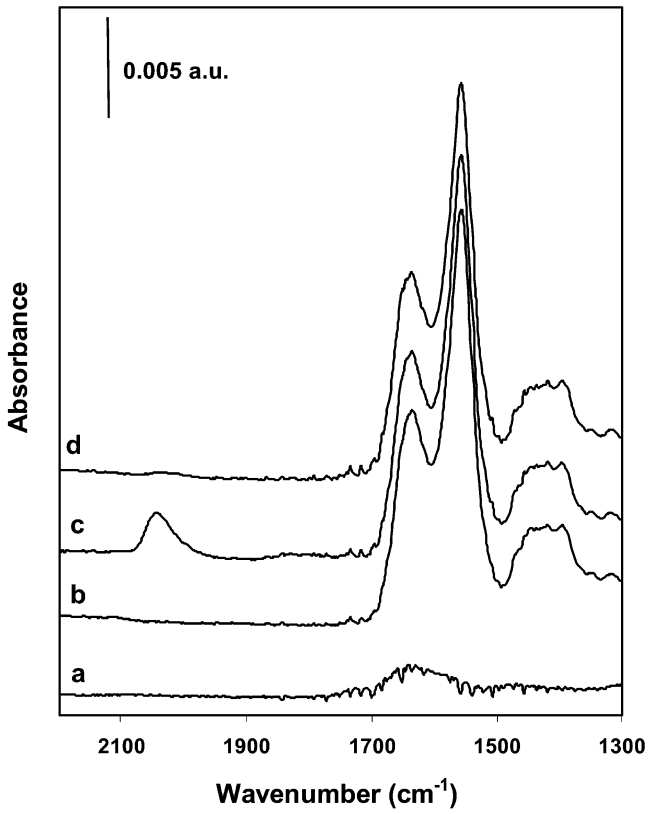

Figure 3. In situ ATR−IR spectra of an alumina film (a) after saturation with water, (b) after exposure to 4.54 μM G4OH/Pt40 solution for 4 h followed by 17 min rinsing with water, (c) after adsorption of CO, and (d) after oxidizing the adsorbed CO with O_2. See text for details.

G4OH/Pt40 injection and exposure for 4 h, the surface was flushed with water. The resulting spectrum (b) clearly shows the amide I (1647 cm^{-1}) and II (1558 cm^{-1}) peaks associated with adsorbed Pt-filled dendrimer. The affinity of G4OH/Pt40 toward alumina is much greater than G4OH. For one, exposure of alumina to similar concentrations of G4OH and G4OH/Pt40 for similar time periods results in a much larger (ca, tenfold higher) surface signal in the case of the latter. This indicates that a higher coverage of dendrimer has been reached in the case of G4OH/Pt40. Furthermore, the dendrimer peak intensities remain constant even after extended rinsing with pure water. Thus, G4OH/Pt40 appears to be irreversibly adsorbed under these conditions.

Both of these observations appear to be consistent with increased van der Waals interactions with alumina that would be expected for Pt-dendrimer nanocomposites as compared with empty dendrimer. Support for this statement comes from estimates of the Hamaker constants for van der Waals interactions between alumina and Pt or PAMAM in an aqueous medium.[38] Using tabulated Hamaker constants in a vacuum for alumina,[39] water,[40] and (as a surrogate for PAMAM-OH) ethanol,[40] we can estimate the Hamaker constants for media 1 and 2 interacting across medium 3 using combining rules.[40] For alumina(1)−Pt(2)−water(3), this constant is calculated to be 10.1×10^{-20} J, while for alumina(1)−ethanol(2)−water(3) it is 0.23×10^{-20} J. These estimates are subject to some error because the combining rules are not very accurate for van der Waals interactions involving water and the fact that a very simple alcohol has been used as the surrogate for the dendrimer. Nevertheless, if these estimates are of the right order of magnitude, they suggest that the van der Waals interaction between alumina and Pt in water is much stronger than that between alumina and PAMAM.

The strong adsorption on alumina has implications for the use of dendrimer-stabilized Pt as a heterogeneous catalyst. First, wet impregnation should be a viable means of delivery to alumina supports, which coincides with what has been observed for SiO_2 supports.[41] Second, G4OH/Pt40 supported on alumina may be a stable material to perform aqueous-phase heterogeneous catalysis. To begin investigating this possibility, we examined the accessibility of the supported dendrimer-stabilized nanoparticles to carbon monoxide, which is a well-known probe of adsorption sites on platinum.

The first step was to determine if the Pt nanoparticle surface remains available for CO adsorption, even in the presence of surrounding dendrimer. Returning to the experiment shown in Figure 3, trace c shows the spectrum obtained upon bubbling CO through the water for 1 h. A prominent peak appears at 2050 cm^{-1} that is associated with terminally adsorbed CO on Pt. The frequency of this feature is identical to that observed previously for adsorption of CO onto a 5 wt % Pt/γ-Al_2O_3 catalyst under the same conditions.[31] We cannot rule out that some possible CO adsorption sites are being blocked by the specific dendrimer interactions with Pt discussed above. However, the similarity between the ν_{CO} frequency on these Pt nanoparticles and those studied previously[31] suggest that the encapsulating dendrimer has little effect on the remaining CO adsorption sites. After purging the system with O_2 for 3 h, the CO surface peak was almost completely removed (Figure 3, trace d). This is also consistent with previous results obtained for the 5 wt % Pt/γ-Al_2O_3 catalyst.[31]

These results clearly show that the small CO molecules can adsorb on the immobilized dendrimer-stabilized Pt nanoparticles. We were, therefore, interested in probing further any similarities (or differences) that might exist between these supported

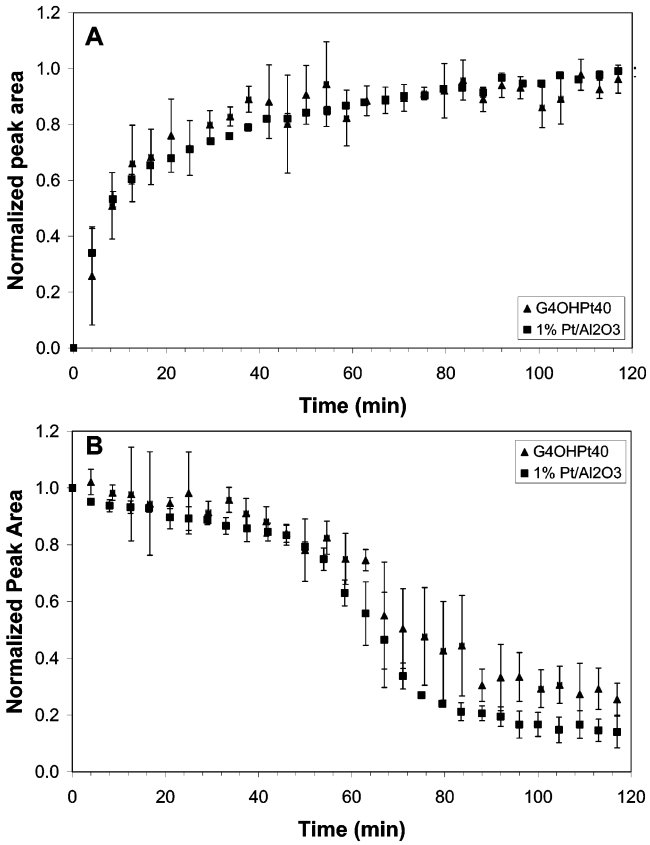

Figure 4. A. Time-dependent infrared signal for adsorbed terminal CO during adsorption on G4OH/Pt40/Al_2O_3 (triangles) and 1 wt % Pt/Al_2O_3 (squares). B. Time-dependent infrared signal for adsorbed terminal CO during N_2 purging on G4OH/Pt40/Al_2O_3 (triangles) and 1 wt % Pt/Al_2O_3 (squares). See text for details.

nanoparticles and a traditional supported Pt catalyst (in this case, 1 wt % Pt on the same γ-Al_2O_3 support). Transient infrared experiments were performed on both materials under the same conditions to compare the rates at which CO adsorbs and is removed from the Pt surface.

Figure 4a shows the transient changes in the ν_{CO} band of adsorbed CO during adsorption onto supported G4OH/Pt40 (triangles) and 1 wt % Pt/γ-Al_2O_3 (squares). Since the thin film preparation for both samples was identical, the same amount of Al_2O_3 was employed for both sets of experiments. Initially, the surfaces were allowed to reach a steady and unchanging signal under flowing N_2-purged water. The N_2 was then switched to CO and spectra were acquired continuously every 5 min. The band intensities have been normalized to the maximum values that were obtained after about 2 h. The vertical bars represent the error obtained for several repetitions of the same experiment. It is apparent from Figure 4a that the transient buildup of adsorbed CO on both surfaces is (to within the error) essentially identical, with the maximum coverage achieved after about 90 min. This suggests that the dendrimer is not limiting the mass transfer of CO to the Pt nanoparticle surface in any significant fashion. The final infrared absorption intensity from the G4OH/Pt40 sample was around tenfold less than the 1% Pt/γ-Al_2O_3. There are two possible explanations for this observation. The most likely is that the loading of Pt in the case of the adsorbed G4OH/Pt40 is much lower than for the 1% Pt/γ-Al_2O_3. While not possible to confirm, a second contributing factor may be that the dendrimer is blocking a significant fraction of adsorption sites.

After reaching the steady-state coverage of adsorbed CO, N_2 was purged through the solution. Figure 4b shows the transient changes in the ν_{CO} band of adsorbed CO during this procedure for G4OH/Pt40 (triangles) and 1 wt % Pt/ γ-Al_2O_3 (squares). The initial time represents the point at which the gas was switched from CO to N_2. The trends in the relative intensity of the ν_{CO} band for both samples were found to be very similar. There is a 50-min period during which the absorption band drops in a linear fashion to around 80% of its initial value. This is followed by a much sharper decrease in the absorption band to a steady state by around 100 min. While the general behavior is very similar, a difference is that after the steady state is achieved, a greater amount of the original adsorbed layer remains for the G4OH/Pt40 (30%) compared to the 1% Pt/γ-Al_2O_3 (15%).

These results show that oxygen is not necessary for desorption and/or removal of the majority of CO from the Pt in the presence of water. In contrast, adsorbed carbon monoxide is very stable on the surface of a dry 1 wt % Pt/γ-Al_2O_3 film that has first been exposed to gas-phase CO before flushing with N_2 (data not shown). Even after 3 h, the adsorbed terminal CO peak remains unchanged in intensity. It is not surprising that CO does not desorb at this temperature on this time scale, given the relatively high CO desorption energies that have been measured for Pt surfaces.[42] The most likely explanation for the removal of adsorbed CO under flowing N_2-purged water is that the CO is being gradually removed through oxidative reaction with adsorbed OH groups from water dissociation. While this is one of the most well-studied electrocatalytic reactions on Pt surfaces,[43] we were unable to find any reports of adsorbed CO oxidation by water *without* potential control. However, it has recently been shown via theoretical studies that such a CO oxidation pathway can occur at room temperature in the absence of electric fields,[44−47] and could even be favored over direct oxidation by adsorbed atomic oxygen. The 50-min induction period behavior that is observed in Figure 4b is easily explained by the fact that the solution-phase CO is only gradually purged by N_2 during this time, thus allowing for constant replenishment of adsorbed CO even as it is being oxidatively removed. Further studies at elevated temperatures in the presence and absence of solution-phase O_2 would be necessary to confirm this interpretation, and are beyond the aim of this paper.

In contrast to the liquid-phase conditions described above, the results are much different when *dry* Al_2O_3-supported G4OH/Pt40 was exposed to CO. An alumina film was exposed to a G4OH/Pt40 solution and extensively washed with water, as described for the experiment in Figure 3. However, the flow cell was then drained of liquid and the film was dried by flowing N_2 over the ATR element for 12 h. The removal of liquid water was confirmed by following the infrared absorbance from liquid water with ATR−IR. Upon exposure of such a dry film to gas-phase CO, no IR peaks associated with adsorbed CO were observed (data not shown). Similar results have also been found for G5OH-encapsulated Pt nanoparticles supported on silica.[41] We believe that this behavior is due to collapsing of the dendrimer shell onto the nanoparticle, which blocks adsorption sites.

This hypothesis is supported by the ATR−IR spectra recorded for the dry Al_2O_3-supported G4OH and G4OH/Pt40 films, which are shown in Figure 5. The upper trace is the spectrum of the dry G4OH/Pt40/Al_2O_3 film, which exhibits the characteristic amide I (1653 cm^{-1}) and amide II (1562 cm^{-1}) peaks. When compared to frequencies obtained for the wet film (cf. Figure 3), the amide I and amide II bands are blue shifted 6 and 4 cm^{-1}, respectively. For comparison, the spectrum of a dry G4OH/Al_2O_3 film is presented as the bottom curve in Figure 5.

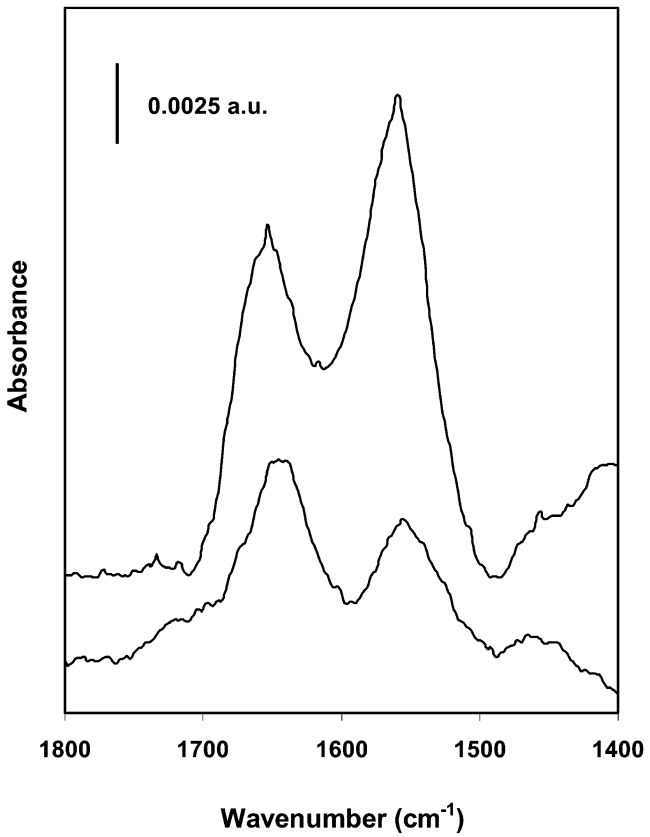

Figure 5. ATR−IR spectra of G4OH (bottom) and G4OH/Pt40 (top) on *dry* alumina films. See text for details.

The film was prepared using the same method and concentrations as described for Figure 2 and dried in flowing N_2 for 12 h. The frequencies of the amide I (1645 cm^{-1}) and amide II (1556 cm^{-1}) bands are blue shifted 8 cm^{-1} and red shifted 4 cm^{-1}, respectively, from the case of a wet film (cf. Figure 2). The amide I/amide II ratios remain roughly the same for both samples when dry, confirming the continuing interaction of the dry dendrimer with the Pt nanoparticle. However, while the frequency of the environmentally sensitive amide I group in both cases increases by about the same amount, the amide II band frequency shifts in opposite directions. Given that this feature is invariant between the two samples in the presence of water, this suggests a new (or increased) interaction of the C−N bond of the dendrimer with the Pt nanoparticle surface. Indeed, similar blue shifts in the amide II vibration have been observed for G4 PAMAM dendrimer-encapsulated Ag and Au nanoparticles, and were attributed to a direct adsorption of the dendrimer branches onto the metal surface.

Conclusion

In conclusion, in situ ATR−IR spectroscopy has been used to examine both bulk solutions and surface adsorption of dendrimers and dendrimer-encapsulated Pt nanoparticles onto wet and dry Al_2O_3. Spectra of G4OH and G4OH/Pt40 solutions reveal that the dendrimer interacts with the Pt nanoparticle through the C═O bonds and that its conformation is effected by the presence of the nanoparticle. While both G4OH and G4OH/Pt40 readily adsorb onto Al_2O_3 in water, the latter is much more strongly (and irreversibly) adsorbed at room temperature. The adsorbed (but still encapsulated) Pt nanoparticles are accessible to dissolved CO, and adsorbed CO can be removed by purging the CO from the liquid with either dissolved O_2 or N_2. The mechanism for this removal is likely via a reaction of CO with adsorbed OH formed from water dissociation. Comparisons with a traditional supported catalyst show that the surrounding dendrimer does not hinder the adsorption of CO on the Pt when liquid water is present. However, under dry conditions the dendrimer appears to completely block any CO adsorption. These results suggest that supported dendrimer-stabilized Pt nanoparticles may be applicable for use as heterogeneous *liquid-phase* catalysts, since the Pt surface may remain accessible to many solution-phase species.

Acknowledgment. This work was funded by a National Science Foundation NIRT award (CTS-0103135). The assistance of Ivelisse Ortiz-Hernandez and Dr. Michael R. Strunk with regard to ATR−IR measurements is also acknowledged.

References and Notes

(1) Tomalia, D. A.; Naylor, A. M.; Goddard, W. A. *Angew. Chem., Int. Ed. Engl.* **1990**, *29*, 138.
(2) Frechet, J. M. *Science* **1994**, *263*, 1710.
(3) Zeng, F.; Zimmerman, S. C. *Chem. Rev.* **1997**, *97*, 1681.
(4) Crooks, R. M.; Lemon, B. I.; Sun, L.; Yeung, L. K.; Zhao, M. *Top. Curr. Chem.* **2001**, *212*, 81.
(5) Zhao, M.; Sun, L.; Crooks, R. M. *J. Am. Chem. Soc.* **1998**, *120*, 4877.
(6) Zhao, M.; Crooks, R. M. *Angew. Chem., Int. Ed. Engl.* **1999**, *38*, 364.
(7) Zhao, M.; Crooks, R. M. *Adv. Mater.* **1999**, *11*, 217.
(8) Zhao, M.; Crooks, R. M. *Chem. Mater.* **1999**, *11*, 3379
(9) Balogh, L.; Tomalia, D. A. *J. Am. Chem. Soc.* **1998**, *120*, 7355.
(10) Esumi, K.; Nakamura, Y.; Suzuki, A.; Torigoe, K. *Langmuir* **2000**, *16*, 7842.
(11) Manna, A.; Imae, T.; Aoi, K.; Odada, M.; Yogo, T. *Chem. Mater.* **2001**, *13*, 1674.
(12) Tomalia, D. A.; Dvornic, P. R. *Nature* **1994**, *372*, 617.
(13) Kanpen, J. W. J.; van der Made, A. W.; de Wilde, J. C.; van Leeuwen, P. W. N. M.; Wijkens, P.; Grove, D. M.; van Koten, G. *Nature* **1994**, *372*, 659.
(14) Haggin, J. *Chem. Eng. News* **1995**, Feb 6, 26.
(15) Jansen, J. F. G. A.; de Brabander-van der Berg, E. M. M.; Meijer, E. W. *Science* **1994**, *266*, 1226.
(16) Garcia, M. E.; Baker, L. A.; Crooks, R. M. *Anal. Chem.* **1999**, *71*, 256
(17) Sayed-Sweet, Y.; Hedstrand, D. M.; Spinder, R.; Tomalia, D. A. *J. Mater. Chem.* **1997**, *7*, 1199.
(18) Strable, E.; Bulte, J. W. M.; Moskovitz, B.; Vivekanandan, K.; Allen, M.; Douglas, T. *Chem. Mater.* **2001**, *13*, 2201.
(19) Niu, Y.; Yeung, L. K.; Crooks, R. M. *J. Am. Chem. Soc.* **2001**, *123*, 6840.
(20) Esumi, K.; Goino, M. *Langmuir* **1998**, *14*, 4466.
(21) Goino, M.; Esumi, K. *J. Coll. Interface. Sci.* **1998**, *203*, 214.
(22) Tokuhisa, Hi.; Zhao, M.; Baker, L. A.; Phan, V. T.; Dermody, D. L.; Garcia, M. E.; Peez, R. F.; Crooks, R. M.; Mayer, T. M. *J. Am. Chem. Soc.* **1998**, *120*, 4492.
(23) Zhao, M.; Tokuhisa, H.; Crooks, R. M. *Angew. Chem., Int. Ed. Engl.* **1997**, *36*, 2596.
(24) Wells, M.; Crooks, R. M. *J. Am. Chem. Soc.* **1996**, *118*, 3988.
(25) Bilznyuk, V. N.; Rinderspacher, F.; Tsukruk, V. V. *Polymer* **1998**, *39*, 5249.
(26) Tokuhisa, H.; Crooks, R. M. *Langmuir* **1997**, *13*, 5608.
(27) Alonso, B.; Moran, M.; Casado, C. M.; Lobete, F.; Losada, J.; Cuadrado, I. *Chem. Mater.* **1995**, *7*, 1440.
(28) Takada, K.; Diaz, D. J.; Abruna, H. D.; Cuadrado, I.; Casado, C.; Alonso, B.; Moran, M.; Losada, J. *J. Am. Chem. Soc.* **1997**, *119*, 10763.
(29) Mirabella, F. M. *Appl. Spectrosc. Rev.* **1985**, *21*, 45.
(30) Pellechia, P. J.; Gao, J.; Gu, Y.; Ploehn, H. J.; Murphy, C. J. *Inorg. Chem.* **2004**, *43*, 1421.
(31) Ortiz-Hernandez, I.; Williams, C. T. *Langmuir*, **2003**, *19*, 2956.
(32) Socrates, G. *Infrared and Raman Characteristic Group Frequencies: Tables and Charts*, 3rd ed.; Wiley: Chichester, 2001.
(33) Barlow, S. M.; Haq, S.; Raval, R. *Langmuir* **2001**, *17*, 3292.
(34) Ishida, K. P.; Griffiths, P. R. *Appl. Spectrosc.* **1993**, *47* (5), 584.
(35) van der Weert, M.; Haris, P. I.; Hennink, W. E.; Crommelin, D. J. A. *Anal. Biochem.* **2001**, *297*, 160.
(36) Pevsner, A.; Diem, M. *Appl. Spectrosc.* **2001**, *55*, 788.
(37) Rahmelow, K.; Hübner, W. A. *Appl. Spectrosc.* **1997**, *51*, 160.
(38) Calculations courtesy of Prof. Harry J. Ploehn.

(39) Lipkin, D. M.; Israelachvilli, J. N.; Clarke, D. R. *Philos. Mag. A* **1997**, *76*, 715.
(40) Israelachvili, J. N. *Intermolecular and Surface Forces*, 2nd ed.; Academic Press: New York, 1992; Ch. 11.
(41) Lang, H.; May, R. A.; Iversen, B. L.; Chandler, B. D. *J. Am. Chem. Soc.* **2003**, *125*, 14832.
(42) For example see: Thomas, V. D.; Schwank, J. W.; Gland, J. L. *Surf. Sci.* **2000**, *464*, 153, and references therein.
(43) For a review see: Vielstich, W. *Encyclopedia of Electrochemistry* **2003**, *2*, 466.
(44) Desai, S.; Neurock, M. *Electrochim. Acta* **2003**, *48*, 3759.
(45) Saravanan, C.; Dunietz, B. D.; Markovic, N. M.; Somorjai, G. A.; Ross, P. N.; Head-Gordon, M. *J. Electroanal. Chem.* **2003**, *554*−*555*, 459.
(46) Narayanasamy, J.; Anderson, A. B. *J. Electroanal. Chem.* **2003**, *554*−*555*, 35.
(47) Gong, X.-Q.; Hu, P.; Raval, R. *J. Chem. Phys.* **2003**, *119*, 6324.